Human Tracking Using Distributed Dual-EKF Filter

Jing Cao[1], Jidong Feng[1], Wanjie Ren[2], Wanfeng Ma[1], Mingran Li[1], and Yuan Xu[1](✉)

[1] School of Electrical Engineering, University of Jinan, Jinan 250022, Shandong, China
xy_abric@126.com

[2] Shandong Institute of Non-metallic Materials, Jinan 250000, Shandong, China

Abstract. Considering the accuracy of the indoor navigation system, an inertial navigation system (INS)/ultra wide band (UWB) technology integrated human tracking using distributed dual-EKF filter will be proposed. In this algorithm, the local data filter we use is composed of four dual-EKF filters to deal with noise more effectively. At the same time, we also take into account the uncertainty of system parameters. It employs the system parameters as the state vector. In the next step, the output of the local filter is input to the main filter for fusion and the best estimate is provided. The experimental results show that this scheme can effectively reduce the positioning error.

Keywords: Iterated dual-EKF · Indoor human localization · Ultra wide band · Inertial measurement unit

1 Introduction

Into the 21st century, with the rapid development of artificial intelligence and wireless Internet, people have put forward higher requirements for navigation performance. We are familiar with the Global Positioning System (GPS) to provide users with positioning services, which greatly promotes the progress of human production and life [4]. However, it is difficult for GPS signals to penetrate solid walls and obstacles, which causes indoor GPS to not work properly. In order to meet the demand for indoor high-precision positioning, how to ensure the accuracy of indoor navigation has become a hot topic [7].

Kalman filter (KF) is a highly efficient recursive filter [5]. KF can be used in any dynamic system with uncertain information to make a basis prediction for the next direction of the system. Once accompanied by various interferences, the Kalman transform can always point out what actually happened [6]. In recent years, KF have been implemented in many different ways. The standard KF is only suitable for linear systems. For nonlinear systems, we can use extended Kalman filter (EKF) for optimal estimationcite [2].

© ICST Institute for Computer Sciences, Social Informatics and Telecommunications Engineering 2022
Published by Springer Nature Switzerland AG 2022. All Rights Reserved
S. Wang et al. (Eds.): IoTCare 2021, LNICST 415, pp. 394–401, 2022.
https://doi.org/10.1007/978-3-030-94182-6_31

Taking into account the positioning error of indoor human tracking, an inertial navigation system (INS)/ultra wide band (UWB) integrated human tracking using distributed dual-EKF filter will be proposed. In this algorithm, the dual-EKF filters is used as the local data fusion filter, which considers the uncertainty of system parameters, it employs the system parameters as the state vector. Next, input the output of the local filter to the main filter for fusion and provide the best estimate. After a lot of experimental verification, it can be determined that this scheme can effectively reduce the positioning error.

The structure of this article is as follows. Robot localization scheme is discussed in Sect. 2. The distributed dual-EKF filtering algorithm is discussed in Sect. 3. In Sect. 4, the performance of distributed dual-EKF algorithm is verified by simulation results. Section 5 summarizes this article.

2 Fusion Model

The fusion model used in this work will be designed in this section. In this work, the time of arrival (TOA)-based UWB is employed, and the two-dimensional (2D) position is considered [3]. Thus, the UWB employed in this work requires at least three UWB reference nodes (RNs) to provide the ranges $r_l, l \in [1, m]$ from the UWB RNs to the UWB blind node (BN). Here, m means the numbers of the UWB RNs. The system chart of the distributed dual-EKF filter is shown in Fig. 1. It includes four local dual-EKF filters and a main filter. The local dual-EKF is employed to provide the $\mathbf{s}(t)^l$ and $\mathbf{P}(t)^l$, and the output of the distributed dual-EKF filter is fused by the main filter.

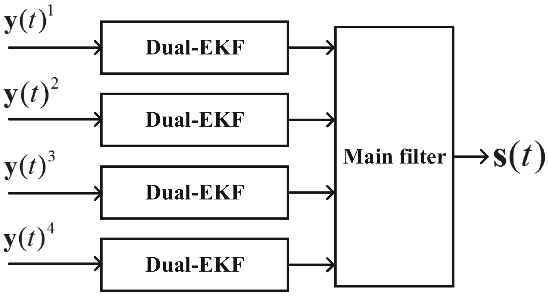

Fig. 1. Structure diagram of distributed dual-EKF filter.

Equation (1) shows the state equation for the local filter in the fusion model, expressing position error and velocity error as state variables.

$$\mathbf{s}(t)^l = \underbrace{\begin{bmatrix} 1 & 0 & \nabla t & 0 \\ 0 & 1 & 0 & \nabla t \\ 0 & 0 & 1 & 0 \\ 0 & 0 & 0 & 1 \end{bmatrix}}_{\mathbf{M}} \mathbf{s}(t-1)^l + \mathbf{w}(t)^l \,, \tag{1}$$

where $\mathbf{s}(t)^l = \left[\nabla x_t^l\ \nabla y_t^l\ \nabla V x_t^l\ \nabla V y_t^l\right]$ is the state vector of the l^{th} local filter at the time index t. At time t, $\left(\nabla x_t^l, \nabla y_t^l\right)$ and $\left(\nabla V x_t^l, \nabla V y_t^l\right)$ represent the position error and velocity error in the x and y directions, respectively. ∇t represents the sample time, $\mathbf{w}(t)^l \sim \mathcal{N}\left(0, \mathbf{Q}^l\right)$ is the process noise.

The measurement equation used in this work can be written as follows according to [1].

$$\begin{aligned}\mathbf{y}(t)^l &= \delta r_{l,t}^2 = (r_{l,t}^I)^2 - (d_{l,t}^U)^2 \\ &= 2\left(x_t^{I,l} - x^l\right)\nabla x_t^l + 2\left(y_t^{I,l} - y^l\right)\nabla y_t^l - \left(\left(\nabla x_t^l\right)^2 + \left(\nabla y_t^l\right)^2\right), \\ &= \mathrm{h}(\mathbf{s}(t)^l) + \gamma_t^l\end{aligned} \tag{2}$$

where $\left(x_t^I, y_t^I\right)$ is the INS position, $\left(x_t^l, y_t^l\right)$ is the l^{th} UWB RN's position, $\gamma(t)^l \sim \mathcal{N}\left(0, \mathbf{R}^l\right)$ is the measurement noise.

3 Distributed Dual-EKF Filter

In this section, the dual-EKF filter, which is used as the local filter based on the model (1) (2) will be designed. Firstly, we rewrite the model (1) (2) as follows:

$$\begin{cases}\mathbf{s}(t)^l = \mathbf{M}(t-1)^l\mathbf{s}(t-1)^l + \mathbf{w}(t)^l \\ \mathbf{y}(t)^l = \mathrm{h}(\mathbf{s}(t)^l) + \gamma_t^l \\ \mathbf{M}(t)^l = \mathbf{M}(t-1)^l + \mathbf{w}^{\mathbf{M}}(t)^l\end{cases}, \tag{3}$$

In this work, the system parameter $\mathbf{M}(t)^l$ is used as the state vector, which means that the uncertain of the system is considered in modified fusion model; the $\mathbf{w}^{\mathbf{M}}(t)^l \sim N\left(0, \mathbf{Q}^{\mathbf{M},l}\right)$ is the noise of the $\mathbf{M}(t)^l$. Based on the model (3), the dual-EKF filter can be designed in the following section.

Firstly, with the initial value $\mathbf{s}(0)^l$ and $\mathbf{P_s}(0)^l$, the $\mathbf{s}(t)^l$ and $\mathbf{P_s}(t)^l$ can be predicted at the time index t via Eqs. (4) (5).

$$\mathbf{s}(t)^l = \mathbf{M}(t-1)^l\mathbf{s}(t-1)^l + \mathbf{w}(t)^l\,, \tag{4}$$

$$\mathbf{P_s}(t)^l = \mathbf{M}(t-1)^l\mathbf{P_s}(t-1)\left(\mathbf{M}(t-1)^l\right)^T + \mathbf{Q}^l\,, \tag{5}$$

where $\mathbf{P_s}(t)^l$ represents the estimation error of $\mathbf{s}(t)^l$. Then, the $\mathbf{s}(t)^l$ and $\mathbf{P_s}(t)^l$ can be updated at the time index t via Eqs. (6) (7) (8).

$$\mathbf{K}\left(t\right)^l = \mathbf{P_s}\left(t\right)^l\left(\mathbf{H}\left(t\right)^l\right)^T[\mathbf{R}\left(t\right)^l + \mathbf{H}\left(t\right)^l\mathbf{P_s}\left(t\right)^l\left(\mathbf{H}\left(t\right)^l\right)^T]^{-1}\,, \tag{6}$$

$$\mathbf{s}\left(t\right)^l = \mathbf{s}\left(t\right)^l + \mathbf{K}\left(t\right)^l[\mathbf{y}\left(t\right)^l - h_t(\mathbf{s}\left(t\right)^l)]\,, \tag{7}$$

$$\mathbf{P_s}\left(t\right)^l = [\mathbf{I} - \mathbf{K}\left(t\right)^l\mathbf{H}\left(t\right)^l]\mathbf{P_s}\left(t\right)^l\,, \tag{8}$$

where $\mathbf{H}\left(t\right)^l = \frac{\partial h_t(\mathbf{s}(t)^l)}{\partial \mathbf{s}(t)^l}$.

Based on the $\mathbf{s}(t)^l$ and $\mathbf{P_s}(t)^l$, the $\mathbf{M}(t)^l$ and $\mathbf{P_M}(t)^l$ can be predicted at the time index t via Eqs. (9) (10).

$$\mathbf{M}(t)^l = \mathbf{M}(t-1)^l + \mathbf{w}^{\mathbf{M}}(t)^l \, , \tag{9}$$

$$\mathbf{P_M}(t)^l = \mathbf{P_M}(t-1) + \mathbf{Q}^{\mathbf{M},l} \, , \tag{10}$$

And then, $\mathbf{M}(t)^l$ and $\mathbf{P_M}(t)^l$ can be updated at the time index t via Eqs. (11) (12) (13).

$$\mathbf{K}\,(t)^{\mathbf{M},l} = \mathbf{P_M}\,(t)^l \left(\mathbf{H}\,(t)^{\mathbf{M},l}\right)^T [\mathbf{R}\,(t)^{\mathbf{M},l} + \mathbf{H}\,(t)^{\mathbf{M},l}\,\mathbf{P_M}\,(t)^l \left(\mathbf{H}\,(t)^{\mathbf{M},l}\right)^T]^{-1} \, , \tag{11}$$

$$\mathbf{M}\,(t)^l = \mathbf{M}\,(t)^l + \mathbf{K}\,(t)^{\mathbf{M},l}\,[\mathbf{y}\,(t)^l - h_t(\mathbf{s}\,(t)^l)] \, , \tag{12}$$

$$\mathbf{P_M}\,(t)^l = [\mathbf{I} - \mathbf{K}\,(\mathrm{t})^{\mathbf{M},l}\,\mathbf{H}\,(\mathrm{t})^{\mathbf{M},l}]\mathbf{P_M}\,(\mathrm{t})^l \, , \tag{13}$$

where $\mathbf{H}\,(t)^{\mathbf{M},l} = \frac{\partial h_t(\mathbf{M}(t)^l)}{\partial \mathbf{M}(t)^l}$.

With the local EKF's output $\mathbf{s}(t)^l$ and $\mathbf{P_s}(t)^l$, the main filter works to provide the optimal output by fusing $\mathbf{s}(t)^l$ and $\mathbf{P_s}(t)^l$ via Eqs. (14) (15).

$$\begin{aligned}\mathbf{s}\,(t) = \mathbf{P_s}\,(t) \Big(&\left(\mathbf{P_s}\,(t)^1\right)^{-1} \mathbf{s}\,(t)^1 + \left(\mathbf{P_s}\,(t)^2\right)^{-1} \mathbf{s}\,(t)^2 + \left(\mathbf{P_s}\,(t)^3\right)^{-1} \mathbf{s}\,(t)^3 \\ &+ \left(\mathbf{P_s}\,(t)^4\right)^{-1} \mathbf{s}\,(t)^4 \Big) \, ,\end{aligned} \tag{14}$$

$$\mathbf{P_s}\,(t) = \left(\left(\mathbf{P_s}\,(t)^1\right)^{-1} + \left(\mathbf{P_s}\,(t)^2\right)^{-1} + \left(\mathbf{P_s}\,(t)^3\right)^{-1} + \left(\mathbf{P_s}\,(t)^4\right)^{-1} \right)^{-1} . \tag{15}$$

4 Experimental Testing

This chapter will design experiments to prove the performance of the proposed algorithm. Firstly, clarify the experimental environment and experimental application equipment. Secondly, compare the proposed method with distributed EKF filters, UWB and INS.

4.1 Experimental Environment

In this experiment, one inertial measurement unit (IMU), one UWB BN and four UWB RNs were used. The author carried a fixed bracket, and the UWB BN was fixed on the bracket. The base station is UWB RN, and UWB RN is fixed at a known point in the test site. The positions of UWB BN and UWB RN should be on the same horizontal plane as possible. The IMU is placed on the feet of the target person in the correct direction. The test environment, experimental equipment and target personnel are shown in Figs. 2 and 3.

Fig. 2. Test environment.

Fig. 3. Experimental equipment and target personnel.

4.2 Performance Analysis of the Proposed Algorithm

In the following, we will discuss the performance of the above algorithm. For a more convenient observation, we compare the positioning error of the proposed method with the distributed EKF filter, UWB and INS. It can be seen that this method can effectively improve accuracy and reduce errors.

Figure 4 shows the estimated path provided by INS, distributed EKF filter and distributed dual-EKF filter, represented by green lines, black dashed lines, purple lines and red lines, respectively. Moreover, the UWB RNs are also shown in the figure. From the figure, one can infer easily that the INS's path has obvious error accumulation, and the UWB has the stable solution. The comparison shows that the distributed EKF filter and the distributed double EKF filter can provide accurate paths. Figure 5 shows the CDF of the positioning error of UWB, distributed EKF filter and distributed dual-EKF filter. Through experiments, it is known that the distributed dual-EKF can better reduce the error. The proposed method's error is about 0.27 m, and that value of the distributed EKF filter is 0.3 m. Moreover, the Table 1 shows the RMSE of the INS, UWB, distributed EKF filter, and distributed dual-EKF filter. It can be confirmed that the distributed dual-EKF proposed in this experiment is better than other algorithms.

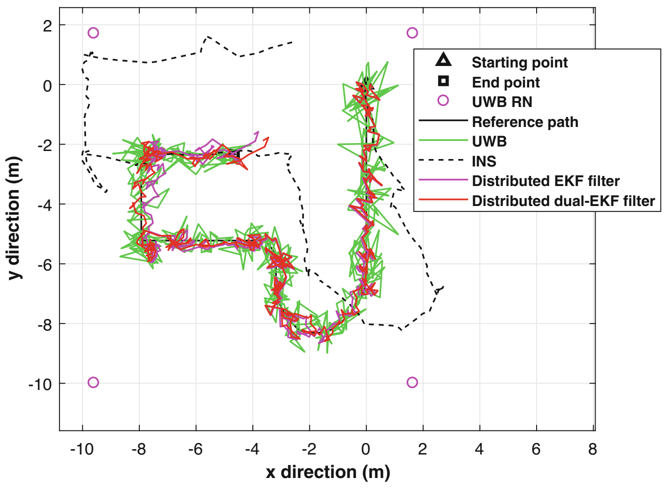

Fig. 4. The estimated path is provided by distributed dual EKF, distributed EKF, UWB and INS.

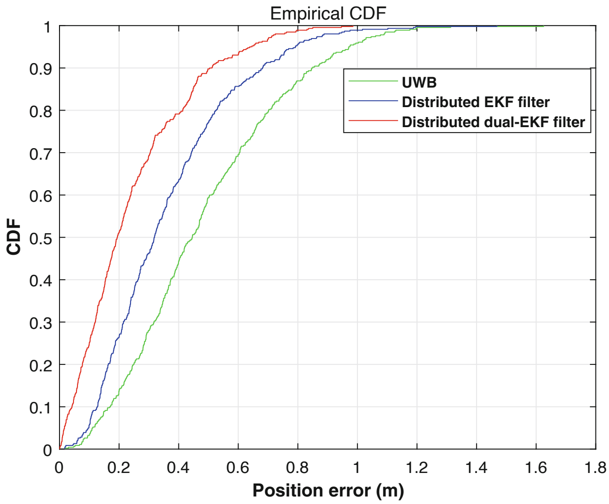

Fig. 5. The CDFs of the distributed dual-EKF, distributed EKF, and UWB.

Table 1. The RMSE(m) generated by INS, UWB, EKF and Dual-EKF

Filter	RMSE	
	East	North
INS	1.62	1.98
UWB	0.39	0.39
EKF	0.36	0.23
Dual-EKF	0.32	0.22

5 Conclusion

The positioning algorithm based on the distributed dual-EKF filter proposed in this paper can better improve the positioning error of human tracking. In this algorithm, it uses four dual-EKF filters as the local data fusion filter, the output of the local filter is used as the input of the main filter, and the fusion provides the best estimate. Through a large number of experiments in this article, it can be proved that the dual-EKF filter can better reduce the error.

Acknowledgements. This work was supported in part by 1) the National Key R&D Program of China 2018AAA0101703, 2) the Shandong Key Research and Development Program under Grant 2019GGX104026, 3) the National Natural Science Foundation of China under Grants 61803175.

References

1. Bu, L., Zhang, Y., Xu, Y.: Indoor pedestrian tracking by combining recent INS and UWB measurements. In: 2017 International Conference on Advanced Mechatronic Systems (ICAMechS), pp. 244–248. IEEE (2017)
2. Jiménez, A.R., Seco, F., Prieto, J.C., Guevara, J.: Indoor pedestrian navigation using an INS/EKF framework for yaw drift reduction and a foot-mounted IMU. In: 2010 7th Workshop on Positioning, Navigation and Communication, pp. 135–143. IEEE(2010)
3. Li, J., Ke, X.: Study on autonomous navigation based on pulsar timing model. Sci. China, Ser. G: Phys. Mech. Astron. **52**(2), 303–309 (2009)
4. Li, X., Zhang, X., Ren, X., Fritsche, M., Wickert, J., Schuh, H.: Precise positioning with current multi-constellation global navigation satellite systems: GPS, GLONASS Galileo and BeiDou. Sci. Rep. **5**(1), 1–14 (2015)
5. Wang, Y., Li, X.: An improved robust EKF algorithm based on sigma points for UWB and foot-mounted IMU fusion positioning. J. Spat. Sci. **66**(2), 329–350 (2021)
6. Xu, Y., Shmaliy, Y.S., Li, Y., Chen, X.: UWB-based indoor human localization with time-delayed data using EFIR filtering. IEEE Access **5**, 16676–16683 (2017)
7. Yang, J., et al.: A height constrained adaptive Kalman filtering based on climbing motion model for GNSS positioning. IEEE Sens. J. **17**(21), 7105–7113 (2017)